to 2012 after acquisition of the approval from the institutional review board of each participating facility. This paper will present the results of the survival survey conducted over 24 months after insertion of the BCNU implant, evaluations during the first 12 months after insertion, and the results of simultaneous BCNU blood level measurements.

Materials and Methods

This study (NPC-08 study) was carried out in compliance with ethical principles based on the Declaration of Helsinki, the study protocol, and Good Clinical Practice. Informed consent for treatment and postoperative follow-up was obtained from all patients. NPC-08 study was registered with ClinicalTrials.gov (number NCT00919737).

I. Patients

The study enrolled patients satisfying all of the following requirements: (1) presence of tumorous lesions in the cerebral parenchyma confirmed by magnetic resonance imaging (MRI), (2) age over 18 and less than 65, (3) Karnofsky performance status (KPS) 60 or over, and (4) histological suspicion of newly diagnosed MGs or recurrent GBM by intraoperative pathological diagnosis. Patients with recurrent GBM were enrolled in the study only when they had received prior conventional radiotherapy. The histopathological diagnosis was reviewed by a central pathological assessment committee separate from the participating facilities to ensure diagnosis by a third party. The required number of cases (24 cases) was defined under the consideration for previously reported adverse events in overseas (CSF leakage etc.). Concerning the required number (24 cases), each recurrent and newly diagnosed MGs should include at least 8 cases to detect the expected side effect.

II. Procedures

A maximum of 8 sheets of BCNU implants were inserted into the removal cavity during surgery (maximum of 61.6 mg BCNU). Re-insertion during the study period was prohibited. On the 14th day following BCNU implant insertion, patients with newly diagnosed MGs received concomitant therapy, i.e., the standard therapy proposed by Stupp et al.[8] involving TMZ (75 mg·m-2day-1) plus radiation (60 Gy) for a maximum period of 6–7 weeks and adjuvant TMZ therapy with 1 cycle consisting of 5-day consecutive TMZ administration (150–200 $mg \cdot m^{-2} day^{-1}$) and a subsequent 23-day cessation. For patients with recurrent GBM, appropriate adjuvant chemotherapy [e.g., chemotherapy with TMZ alone or TMZ plus Interferon- (INF-β)] was permitted (Fig. 2).

In this study, first we evaluated the status of the occurrence of adverse events carefully in a small number of patients (6 patients) at the efficacy and safety evaluation committee, and then, based on the judgment of the committee, we moved to a multicenter study with larger sample size.

Methods and Statistical Analyses

For efficacy evaluation, the overall survival (OS) rate at 24 months after insertion, median overall survival (mOS) period, and progression-free survival (PFS) rate at 12 months after insertion of BCNU implants were calculated by the Kaplan-Meier method. The following two population groups were an effective analysis set and are defined as a full analysis set (FAS) unless otherwise specifically noted:

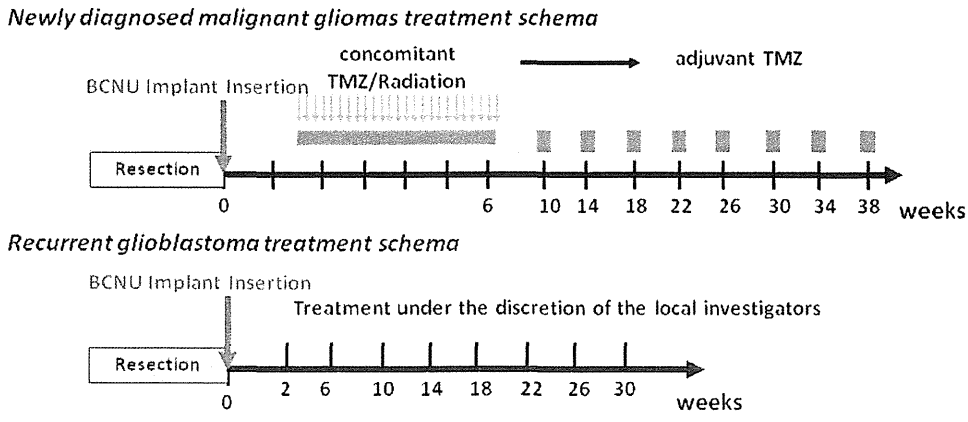

Fig. 2 Treatment schema. TMZ: temozolomide.

(a) An FAS group consisting of all subjects enrolled in the clinical study excluding those who never underwent implantation with the present formulation and (b) A group verified to have GBM/other GBM (non-GBM) based on the central pathological diagnosis.

To evaluate PFS, tumor progression was rated based on the following criteria: the tumor was classified as progressive if its major diameter multiplied by its vertical dimension (short minor diameter) showed a > 25% increase in comparison with the preceding image showing the minimum value for each parameter or if any new lesion(s) appeared (McDonald criteria). Evaluation of MRIs was carried out by the efficacy and safety evaluation committee in accordance with the McDonald criteria, and the evaluators were blinded to the background variables of the subjects. For efficacy analysis, the OS rate, mOS period, PFS rate, and median PFS period were determined by the Kaplan-Meier method, and 95% confidence intervals (95% CIs) were calculated for each parameter. The OS time and PFS time were not analyzed in this study.

However, when OS and PFS were lower than 50% up to the cutoff time in a given patient population, a median survival period was calculated. One month was defined as 30 days, and 1 year was defined as 360 days. To determine safety profiles, adverse events and abnormal changes in laboratory parameters were evaluated until the 12th month in all patients who received BCNU implants in accordance with the National Cancer Institute Common Terminology Criteria for Adverse Events (CTCAE) version 3.0.

Adverse events were classified in accordance with the Medical Dictionary for Regulatory Activities Japanese translation (MedDRA/J) version 14.0. The number of patients who experienced each event and the incidence of each event were analyzed in relation to severity. All evaluations performed by attending physicians were reviewed by the efficacy and safety evaluation committee.

For pharmacokinetic analysis, BCNU levels in the blood were measured periodically (before insertion and 3–6 hours, 24 hours, 72 hours, or 168 hours after insertion). Validation and BCNU measurement in blood samples were carried out by liquid chromatography-tandem mass spectrometry (LC/MS/MS) at Celerion Inc (Lincoln, Nebraska, USA).

Validation of the quantification method employed in this study confirmed good linearity of BCNU and the internal standard (d8-BCNU) within the range of quantification (2.00–100 ng/mL) (≥ 0.9952). The lower limit of quantitation was set at 2.00 ng/mL.

Table 1 Patient characteristics

		Newly diagnosed malignant gliomas (n = 16)	Recurrrent malignant gliomas (n = 8)
Age (years)	Mean	46.6	42.9
	SD	14.09	14.57
	Min	21	25
	Median	49.5	41
	Max	63	63
Male/Female		8/8	4/4
Preoperative tumor sizes	Mean	23.0	16.9
	SD	15.0	10.5
	Min	2.0	3.5
(cm^2)	Median	22.5	22.6
	Max	62.4	26.3
Rate of tumor resection	Mean	91.9	87.3
	SD	8.5	17.0
	Min	80.0	55.0
(%)	Median	92.5	95.0
	Max	100	100
Number of BCNU implants	Mean	7.7	7.9
	SD	0.87	0.35
	Min	5.0	7.0
(sheets)	Median	8.0	8.0
	Max	8	8
Pre-insertion KPS score	60	1 (6.3)	0 (0.0)
	70	1 (6.3)	2 (25.0)
	80	4 (25.0)	1 (12.5)
(%)	90	7 (43.8)	3 (37.5)
	100	3 (18.8)	2 (25.0)
	≤70	2 (12.5)	2 (25.0)
	80≤	14 (87.5)	6 (75.0)
1st/2nd recurrence	1st	–	6 (75.0)
	2nd	–	2 (25.0)
History of medical treatment for tumor	Yes	–	7 (87.5)
	No	–	1 (12.5)

KPS: Karnofsky performance status.

Results

Table 1 outlines the patient characteristics. During this study, BCNU implants were inserted in a total

of 24 patients. At intraoperative pathological consultations, these 16 newly and 8 recurrent patients were diagnosed as MGs or GBM. However, after the central pathological diagnoses of the 16 newly diagnosed MGs during the central review were GBM in 9 cases and other tumors in 7 cases (3 cases of anaplastic oligodendroglioma, 2 cases of oligodendroglioma, and 1 case each of anaplastic ganglioglioma and oligoastrocytoma). Of the 8 recurrent GBMs, the diagnoses were GBM in 4cases and other tumors in 4 cases (1 case each of anaplastic oligodendroglioma, anaplastic oligoastrocytoma, anaplastic astrocytoma, and high-grade glioma).

In 6 of 24 patients, whole blood BCNU levels were measured. The ages (mean ± SD) were 45.4 ± 14.05 years, 46.6 ± 14.09 years, and 42.9 ± 14.57 years in the entire population, patients with newly diagnosed MGs, and patients with recurrent MGs, respectively. There were 12 male (50.0%) and 12 female (50.0%) patients, indicating no gender bias. The duration of illness were 16.7 ± 28.88 months, 5.7 ± 15.07 months, and 38.8 ± 37.71 months in the entire population, patients with newly diagnosed MGs, and patients with recurrent MGs, respectively. The preoperative tumor sizes were 21.0 ± 13.8 cm^2, 23.0 ± 15.0 cm^2, and 16.9 ± 10.5 cm^2 in the entire population, patients with newly diagnosed MGs, and patients with recurrent MGs, respectively. The median tumor sizes were 22.6 cm^2, 22.5 cm^2 and 22.6 cm^2 in the entire population, patients with newly diagnosed MGs, and patients with recurrent MGs, respectively. The rates of tumor resection were 90.3 ± 11.8%, 91.9 ± 8.5%, and 87.3 ± 17.0% in the entire population, patients with newly diagnosed MGs, and recurrent MGs, respectively. The rates of median tumor resection were 92.5%, 92.5%, and 95.0% in the entire population, patients with newly diagnosed MGs, and patients with recurrent MGs, respectively. The number of patients with a pre-insertion KPS score over 80 was 20 (83.3%) in the entire population, 14 (87.5%) in patients with newly diagnosed MGs, and 6 (75.0%) in patients with recurrent MGs. Of the recurrent MGs patients, recurrence occurred once in 6 cases (75.0%) and twice in 2 cases (25.0%). All recurrent MG patients received conventional radiotherapy (local), and 7 of these patients (87.5%) had a history of medical treatment for the tumor. Tumor resection in the newly diagnosed MG patients was partial removal: 9 cases (56.3%) and total removal: 7 cases (43.7%). Tumor resection in the previous treatment of recurrent MG patients was biopsy: 2 cases (25.0%), partial removal: 4 cases (50.0%), and total removal: 2 cases (25.0%). In this study, the period from the first operation to the second was less than 1 year in 4 recurrent MG patients (50.0%). Eight sheets of BCNU implants were inserted in 21 of 24 patients. One patient each received 7, 6, and 5 sheets.

After surgery, standard TMZ plus conventional radiotherapy was utilized for all newly diagnosed MG patients (n = 16). For recurrent MG patients, TMZ alone (n = 7) or TMZ plus INF-β therapy (n = 1), BEV therapy (n = 2), or IMRT therapy (n = 1) was utilized.

I. Efficacy

Using the Kaplan-Meier method, OS rates at 12 and 24 months for patients with newly diagnosed MGs were 100% and 68.8%, respectively (95% CI: 40.5–85.6%). The mOS in this group could not be calculated (Fig. 3). For patients with recurrent MGs, the OS rate at 6 months was 87.5% (95% CI: 38.7–98.1%), the OS rate at 12 months was 62.5% (95% CI: 22.9–86.1%), the OS rate at 24 months was 25.0% (95% CI: 3.7–55.8%), and the mOS was 12.0 months (361 days) (Fig. 3). In subgroup analysis of patients according to histological type, the 16 patients with newly diagnosed MGs were divided into the GBM group and the non-GBM group. In the GBM group (n = 9), the OS rate at 24 months and the mOS were 44.4% (95% CI: 13.6–71.9%) and 20.2 months, respectively. In the non-GBM group (n = 7), the OS rate was 100%. For patients with recurrent MGs, the OS rate at 12 months and the mOS were 50.0% (95% CI: 5.8–84.5%) and 8.6 months, respectively, in the GBM group (n = 4). In the non-GBM group (n = 4), the OS rate was 75.0% (95% CI: 12.8–96.1%) and the mOS was 12 months. According to the Kaplan–Meier method, the PFS rate at 6 months was 75.0% (95% CI: 46.3–89.8%) and

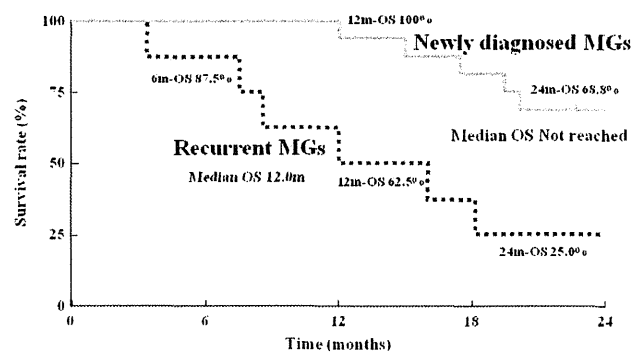

Fig. 3 Kaplan-Meier curve of survival period/rate. MGs: malignant gliomas, OS: overall survival rate, m: months, 6m-OS: the overall survival rates at 6 months, 12m-OS: the overall survival rates at 12 months, 24m-OS: the overall survival rates at 24 months.

that at 12 months was 62.5% (95%CI: 34.9–81.1%) in patients with newly diagnosed MGs (Fig. 4). When this group was subdivided, the PFS rate at 12 months was 55.6% (95% CI: 20.4–80.5%) in the GBM group and 71.4% (95% CI: 25.8–92.0%) in the non-GBM group. For patients with recurrent MGs, the PFS rate at 6 months was 37.5% (95% CI: 8.7–67.4%), the PFS rate at 12 months was 25.0% (95% CI: 3.7–55.8%), and the median PFS was 170 days (Fig. 4). When this group was subdivided, the PFS rates at 6 monthsand 12 months were both 25.0% (95% CI: 0.9–66.5%) in the GBM group and 50.0% (95% CI: 5.8–84.5%) in the non-GBM group. Figure 5 shows gadolinium contrast-enhanced T_1 MRIs before insertion, within 3 days of insertion, and 6 months and 12 months after insertion of BCNU implants in a patient with recurrent GBM (first relapse). A tumor, 5 cm in size, was noted in the left frontal lobe, and 8 sheets of the BCNU implant were inserted. Subsequently, TMZ alone (220–260 mg/day) was applied for 9 cycles. Even at 12 months after insertion, there was no tumor growth or any other changes observable on MRI images.

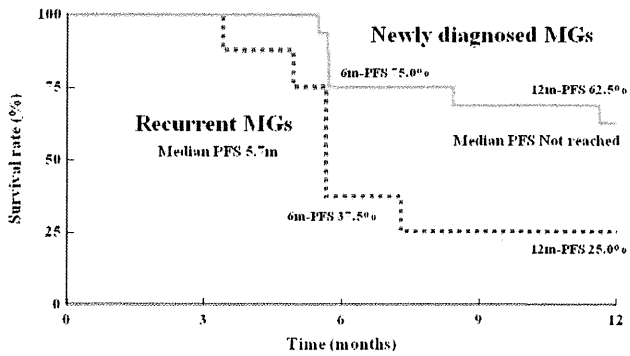

Fig. 4 Kaplan-Meier curve of progression-free survival period/rate (judged by the efficacy and safety evaluation committee). MGs: malignant gliomas, PFS: progression-free survival rate, m: months, 6m-PFS: progression-free survival rate at 6 months, 12m-PFS: progression-free survival rate at 12 months.

During this study, non-responders to TMZ received either BEV therapy (1 newly diagnosed GBM patient and 1 recurrent GBM patient) or IMRT therapy (1 recurrent anaplastic astrocytoma patient). BEV therapy for the newly diagnosed GBM patient involved 5 cycles of treatment (330 mg/day) after recurrence at 8.4 months after insertion of BCNU implants. The patient died 12 months (362 days) after insertion of the BCNU implants. BEV therapy for the second recurrence GBM patient involved 10 cycles of treatment (500 mg/day) at 5.7 months after insertion of the BCNU implants. The patient died at 18.2 months (546 days) after insertion of the BCNU implants. IMRT therapy was applied at a dose of 60 Gy to the enhanced area and 50 Gy to the area around the lesion after the

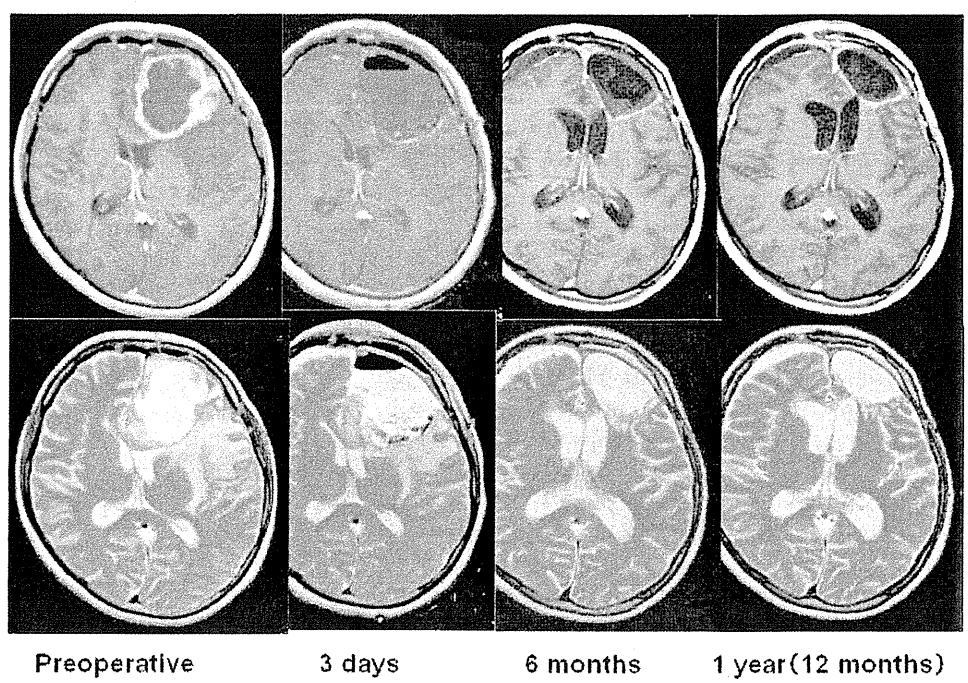

Fig. 5 Time course of magnetic resonance (MR) imaging findings (1st relapse of recurrent glioblastoma), axial gadolinium contrast-enhanced T_1-weighted MR images (*upper row*), and T_2-weighted MR images (*lower row*).

second recurrence at 7.3 months after insertion of the BCNU implants. The patient died at 16.1 months (483 days) after insertion of the BCNU implants.

II. Safety

Adverse events were noted in 24 of 24 (100%) patients who received BCNU implants and adverse events attributable to BCNU implants were 13 of 24 patients (54.2%). Major adverse events (over 20%, Table 2) listed in descending order of incidence were fever (18 cases, 75.0%); alopecia (16 cases, 66.7%); constipation (14 cases, 58.3%); headache (13 cases, 54.2%); nausea (12 cases, 50.0%), wound complication and leukocytopenia (11 cases each, 45.8%); brain neoplasm (10 cases, 41.7%); vomiting, malaise, brain edema, and lymphopenia (9 cases each, 37.5%); anorexia and hemiparesis (8 cases each, 33.3%); insomnia (7 cases, 29.2%); aphasia, seizure, and increase in blood creatine phosphokinase (CPK; 6 cases each, 25.0%); and pruritus, facial swelling, radiation-induced skin injury, and weight loss (5 cases each, 20.8%). Of these adverse events, severe events (grade 3) included brain neoplasm (7 cases, 29.2%), hemiplegia (6 cases, 25.0%), brain edema (4 cases, 16.7%), and aphasia (3 cases, 12.5%). Adverse, life-threatening events or those causing disabilities (grade 4) included tumor progression (3 cases, 4.2%).

Within 12 months (360 days) of BCNU implant insertion, 3 patients died from tumor progression. None of the deaths had causal relationships with the investigational drug. Within 24 months of BCNU implant insertion, 6 patients died in addition to the above-mentioned 3 patients (9 deaths in total). The cause of death was progressive disease (PD) in 5 cases (2 newly diagnosed MGs and 3 recurrent MGs) and respiratory failure in 1 case (newly diagnosed MG). None of these deaths had causal relationships with the investigational drug.

Frequently noted adverse events attributable to BCNU implants (adverse reactions, Table 3) were brain edema (6 cases, 25.0%); fever and lymphocytopenia (3 cases each, 12.5%); and nausea, vomiting, headache, hemiparesis, anorexia, and increase in alanine aminotransferase (ALT; 2 cases each, 8.3%). None of these adverse reactions were rated as grade 4 or worse. There were 6 cases of grade 3 events in 5 of 24 patients (20.8%) including brain edema (2 cases), hemiparesis (2 cases), increase in ALT (1 case), and increase in CPK (1 case). None of the patients experienced convulsion, poor wound healing, infection, meningitis, or hydrocephalus as an adverse reaction. The adverse reactions listed above appeared within 3 months of BCNU implant insertion.

Among the patients who did not respond to TMZ

Table 2 Number of patients (%) who experienced adverse events according to Common Terminology Criteria for Adverse Events (CTCAE) grade (events with an incidence over 20%)

System organ class/event name	Cases (%) (n = 24)			
	All grades		Grade 3 or higher	
All adverse events	24	(100.0)	19	(79.2)
Gastrointestinal disorders				
Nausea	12	(50.0)		–
Constipation	14	(58.3)		–
Vomiting	9	(37.5)		–
General disorders and administration site conditions				
Malaise	9	(37.5)		–
Fever	18	(75.0)	1	(4.2)
Injury, poisoning, and procedural complications				
Wound complication	11	(45.8)		–
Nervous system disorders				
Aphasia	6	(25.0)	3	(12.5)
Headache	13	(54.2)		–
Brain edema	9	(37.5)	4	(16.7)
Hemiparesis	8	(33.3)	6	(25.0)
Seizure	6	(25.0)	1	(4.2)
Psychiatric disorders				
Insomnia	7	(29.2)		–
Metabolism and nutrition disorders				
Anorexia	8	(33.3)		–
Skin and subcutaneous disorders				
Pruritus	5	(20.8)		–
Facial swelling	5	(20.8)		–
Alopecia	16	(66.7)		–
Radiation-induced skin injury	5	(20.8)		–
Neoplasms (benign, malignant, and unspecified)				
Brain neoplasm	10	(41.7)	7	(29.2)
Investigations				
Lymphopenia	9	(37.5)	2	(8.3)
Blood creatine phosphokinase increased	6	(25.0)	2	(8.3)
Weight loss	5	(20.8)		–
Leukocytopenia	11	(45.8)	2	(8.3)

MedDRA/J Version 14.0. Event name: The same event name seen in the same patient was counted as one case. If severity differed between multiple episodes of the same event, then the most severe episode was selected. System organ class: If there were multiple event names within the same system organ class in the same patient in one line, the patient was counted as one. Incidence (%) = No. of patients developing the event / All patients studied × 100.

Table 3 Number of patients (%) who attributable to BCNU implants according to Common Terminology Criteria for Adverse Events (CTCAE) grade

System organ class/event name	Cases (%) (n = 24)			
	All grades		Grade 3 or higher	
All adverse reactions	13	(54.2)	5	(20.8)
Gastrointestinal disorders				
Nausea	2	(8.3)		–
Abdominal discomfort	1	(4.2)		–
Vomiting	2	(8.3)		–
General disorders and administration site conditions				
Hypothermia	1	(4.2)		–
Fever	3	(12.5)		–
Edema	1	(4.2)		–
Nervous system disorders				
Hyperesthesia	1	(4.2)		–
Memory disorder	1	(4.2)		–
Aphasia	1	(4.2)		–
Heterotropia	1	(4.2)		–
Headache	2	(8.3)		–
Homonymous hemianopsia	1	(4.2)		–
Urinary incontinence	1	(4.2)		–
Brain edema	6	(25.0)	2	(8.3)
Monoparesis	1	(4.2)		–
Hemiparesis	2	(8.3)	2	(8.3)
Hemiplegia	1	(4.2)		–
Reproductive system and breast disorders				
Irregular menstruation	1	(4.2)		–
Metabolism and nutrition disorders				
Anorexia	2	(8.3)		–
Investigations				
C-reactive protein increased	1	(4.2)		–
Alanine aminotransferase increasd	2	(8.3)	1	(4.2)
Lymphocyte decreased	3	(12.5)		–
Platelet decreased	1	(4.2)		–
Blood creatine phosphokinase increased	1	(4.2)	1	(4.2)
Leukocyte increased	1	(4.2)		–

※ MedDRA/J Version 14.0. Event name: the same event name seen in the same patient was counted as one case.

and who received BEV therapy (1 newly diagnosed GBM patient and 1 recurrent GBM patient) or IMRT therapy (1 recurrent anaplastic astrocytoma patient), leukocytopenia (grade 2) was noted in a patient who underwent BEV therapy and alopecia (grade 2) and malaise (grade 2) were noted in a patient who underwent IMRT therapy.

III. Pharmacokinetics

BCNU levels in whole blood were measured in 6 of the patients who received BCNU implants. The age of these 6 patients (mean ± SD) was 45.5 ± 15.7 years (21–61 years), body weight was 59.2 ± 14.2 kg (42.9–77.1 kg), median number of BCNU implant sheets inserted was 8 sheets (5–8 sheets: 8 in 4 cases, 7 and 5 in 1 case each), and the administration of BCNU at a median dose level were 61.6 mg (38.5–61.6 mg). As shown in Fig. 6, BCNU levels reached a peak approximately 3 hours after insertion and ranged from 6.49 ng/mL to 19.4 ng/mL (10.19 ± 4.77 ng/mL). After 24 hours, levels were in the vicinity of or below the lower limit of quantification (2.00 ng/mL).

Discussion

This study (NPC-08 study) was designed to evaluate the efficacy, safety, and pharmacokinetics of BCNU implants with chemotherapy (including TMZ) and radiotherapy for Japanese patients with newly diagnosed MGs or recurrent GBM (under conditions indicated for BCNU in USA and Europe). Of the 24 patients who received BCNU implants (newly diagnosed MG, 16 cases; recurrent MG, 8 cases), the survival rate for patients with newly diagnosed

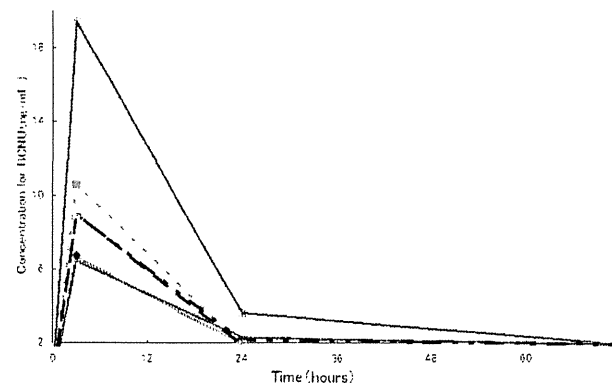

Fig. 6 Time course of BCNU levels in whole blood. Six Japanese patients with malignant gliomas received the maximum blood concentration of BCNU at about 3 hours after implant placement was 19.4 ng/mL. The lower limit of quantitation (2.00 ng/mL).

MGs was 100.0% at 12 months and 68.8% at 24 months, making it impossible to calculate the median survival time in this group. These results were superior those of placebo-controlled double-blind comparative studies[3,4] conducted in USA and Europe in which the OS rate at 12 months was 59.2% (95% CI: 50.4–68.0%) and the mOS was 13.8 months (95% CI: 12.1–15.1 months). However, these studies from USA and Europe were not combined therapy involving TMZ plus radiotherapy for newly diagnosed MGs cases. In NPC-08 study, combined TMZ plus radiotherapy was applied to all patients with newly diagnosed MGs after insertion of BCNU implants. According to previous reports[9–13] examining combined TMZ plus radiotherapy after insertion of BCNU implants, the OS rate at 12 months and 24 months was 56.8–81.0% and 13.0–47.0%. Furthermore, the OS rate at 6 months with recurrent MG was 87.5% in NPC-08 study. According to a clinical study by Brem et al.,[2] the OS rate at 6 months in patients with recurrent MG was 60%. Thus, although the number of patients studied was small, the results of the NPC-08 study were comparable to the results of USA and European studies.

Potential adverse effects of BCNU implants were noted in 13 of 24 patients (54.2%). Severe adverse reactions were noted in 5 of 24 patients (20.8%), although none were live threatening. Important adverse events requiring close attention include brain edema, seizure, poor wound healing, infection, headache, hemiparesis, meningitis, and hydrocephalus according to clinical reports from USA and Europe. We compared the adverse event data in NPC-08 study with the data from three placebo-controlled double-blind comparative studies conducted in USA and Europe (Table 4).

The incidence of Brain edema was higher in the NPC-08 study (25.0%, 6/24 patients) than that in the double-blind studies (4.9%, 12/246 patients). However, there was no significant difference between the BCNU implant group and the placebo group regarding brain edema on grade 3 or worse in the double-blind studies. Brain edema can also be caused by tumor resection, MGs themselves, dose of steroid and so on, therefore, the expression of the brain edema is necessary to be careful, it is necessary to consider the administration of steroid drug. In this study, brain edema of any CTCAE grade occurred in 6 of 24 patients. There were no patients with brain edema of CTCAE grade 4. Two patients developed brain edema of CTCAE grade 3. These two patients were not from a specific facility. We examined the occurrence rate of brain edema by each patient's background in the Japanese studies, but were unable to find any tendency due to the small sample size. Nearly 700 patients were enrolled in foreign studies. Among those patients, 3.8% (26/676) developed brain edema of any CTCAE grade, and 1.9% (12/676) developed brain edema of CTCAE grade 3 or 4. On the other hand, the total number of patients enrolled in the Japanese study was small (24 patients). We consider that this small number of patients (denominator) may have contributed to a large difference; i.e., in the present case, higher rate of brain edema occurrence than in foreign studies. In addition, we infer that one of the reasons that brain edema were more often observed in Japan than in foreign countries is as follows: the protocol for the Japanese study has described "brain edema, convulsion, cerebrospinal fluid (CSF) leakage, and limited hypofunction" as notable adverse events that were reported in foreign studies, and requested investigators and clinical research coordinators to carefully watch for these adverse events. This may have encouraged physicians to conduct CT/MRI testing more frequently than is required in the protocol, leading to observation of higher occurrence rate of brain edema. In summary, although the occurrence rate of brain edema was higher in the Japanese study than in the foreign studies, it is difficult to determine whether the Japanese patients are more likely to develop brain edema than the foreign patients because of the small number of the Japanese patients enrolled in this study. This question should be addressed in future studies. Seizure is one of the complications of brain tumors and neurosurgical interventions, and its incidence differed little between NPC-08 study and the combined double-blind studies. There was no difference between the BCNU implant group and the placebo group in terms of overall incidence or incidence of seizure grade 3 or worse. One of the 3 double-blind studies, Brem et al.[2] reported that the median day of onset of seizures was faster in the BCNU implant group (3.5 days) than in the placebo group (55.5 days) (Wilcoxon test: $P = 0.01$). In the NPC-08 study, the median day of onset of seizures was 91.5 days.

Since the number of patients studied was small, these results were not clear that the day of onset of seizures was tended to be faster by BCNU implant. However, it is necessary to consider the administration of anticonvulsant drugs. None of the patients was experienced poor wound healing after craniotomy as adverse reactions in the NPC-08 study. In the combined double-blind studies, the incidence of poor healing was slightly higher in the BCNU implant group (7.3%, 18/246 patients) than in the placebo group (3.2%, 8/248 patients). Therefore, the expression of poor wound healing is necessary to

Table 4 Comparison of the number of patients (incidence) who experienced major adverse reactions in the NPC-08 study and in the combined double-blind comparative studies

System organ class/Event name	The NPC-08 study						Double-blind studies[2,10,13]									
	All grades						All grades						Placebo			
	All grades		Grade 3		Grade 4		All grades		Grade 3		Grade 4		All grades		Grade 3		Grade 4	
Total patients	24						246						248					
Brain edema	6	(25.0)	2	(8.3)	–		12	(4.9)	2	(0.8)	3	(1.2)	12	(4.8)	4	(1.6)	2	(0.8)
Seizure		–		–	–		31	(12.6)	7	(2.8)	2	(0.8)	39	(15.7)	11	(4.4)	2	(0.8)
Major seizure		–		–	–		1	(0.4)		–		–	2	(0.8)		–	1	(0.4)
Poor healing		–		–	–		18	(7.3)	4	(1.6)		–	8	(3.2)	1	(0.4)		–
Infection		–		–	–		13	(5.3)	2	(0.8)	3	(1.2)	16	(6.5)	2	(0.8)		–
Headache	2	(8.3)		–	–		28	(11.4)	8	(3.3)		–	22	(8.9)	8	(3.2)	1	(0.4)
Hemiplegia	1	(4.2)		–	–		24	(9.8)	5	(2.0)		–	34	(13.7)	15	(6.0)		–
Monoparesis	1	(4.2)		–	–			–		–		–		–		–		–
Hemiparesis	2	(8.3)	2	(8.3)	–			–		–		–		–		–		–
Meningitis		–		–	–		5	(2.0)	2	(0.8)		–	1	(0.4)		–		–
Hydrocephalus		–		–	–		2	(0.8)	1	(0.4)	1	(0.4)	1	(0.4)		–		–

MedDRA/J Version 14.0. Event name: The same event name seen in the same patient was counted as one case. If severity differed between multiple episodes of the same event, then the most severe episode was selected. Incidence (%) = No. of patients who experienced adverse reaction/all patients studied × 100.

be careful. Infection and meningitis were not observed in the NPC-08 study. In the combined double-blind studies, the overall incidence of this event and the incidence of grade 3 or worse differed little between the BCNU implant group and the placebo group, and the incidence was also high in the placebo group.

The incidence of headache was not high in the NPC-08 study (8.3%) and differed little between the BCNU implant group and the placebo group. The incidence of hemiparesis was slightly higher in the combined double-blind studies. Hydrocephalus did not develop in any patient in the NPC-08 study. In the combined double-blind studies, the incidence of hydrocephalus was approximately 0.8% in the BCNU implant group, which was comparable to its incidence in the placebo group. All of the important adverse events discussed above were symptoms accompanying a brain tumor or surgical resection of the tumor.

For pharmacokinetic analysis, BCNU levels in the blood were measured at multiple time points after surgery. The administration of BCNU at a median dose level of 61.6 mg (38.5–61.6 mg) to 6 patients caused a mean peak BCNU level of 10.19 ng/mL. BCNU has been administered intravenously and inserted into the removal cavity for the treatment of brain tumors in USA and Europe. According to a report[14] describing the pharmacokinetics of intravenous BCNU injection, the peak BCNU level in the blood averaged 6.2 μg/mL, whereas the peak level following insertion in the brain averaged 0.01 μg/mL.

Thus, the BCNU level in the blood after insertion into the brain was much lower (1/600) than that after intravenous injection, and BCNU disappears from the blood almost completely within 24 hours of insertion into the brain.

Systemic administration of BCNU often induces severe adverse events such as leucopenia and thrombocytopenia. Insertion of BCNU implants into the brain is expected to markedly reduce systemic adverse events as compared with intravenous BCNU.

Taken together, these results indicate that when insertion of BCNU implants into the brain (maximum of 8 sheets containing a maximum of 61.6 mg BCNU) was followed by chemotherapy or radiotherapy in patients with newly diagnosed or recurrent MGs, there are no major safety concerns associated with the use of BCNU implants. The BCNU implant is now recommended as a treatment option along with the surgical resection of MGs on the basis of established treatment guidelines. The data from this clinical study was comparable to previous data from USA and Europe with respect to efficacy and safety. Therefore, from a risk/benefit viewpoint, the use of BCNU implants is recommended.

Acknowledgments

The authors are indebted to many professionals involved in the NPC-08 study including neurosurgeons; physicians specializing in radiological treatment, chemotherapy, or pathological diagnosis; nurses; pharmacists; clinical trial coordinators; and many others in addition to the 24 patients who participated in the study. The authors greatly appreciate their support. Special thanks to the NPC-08 study group.

Clinical investigators

(a) Saitama Medical University International Medical Center: Kenji Wakiya and Tomonari Suzuki; (b) Kitano Hospital: Hiroki Toda, Jun Takahashi, Tsuyoshi Ota, Namiko Nishida, Hideki Hayashi, Yoshitaka Kurosaki, Koichi Fujimoto, and Taichi Ikedou; (c) Graduate School of Biomedical & Health Sciences, Hiroshima University: Yoshinori Kajiwara, Taiichi Saitou, Yousuke Watanabe, and Takeshi Takayasu; (d) Tohoku University Graduate School of Medicine: Yukihiko Sonoda, Ryuta Saito, Mika Watanabe, and Hisanori Ariga; (e) Dokkyo Medical University Hospital: Yoshifumi Okada, Masahiro Ogino, Kazushige Itoki, Yoshihiro Abe, and Kanae Mochiki; (f) Faculty of Medicine, University of Tsukuba: Akira Matsumura, Shingo Takano, Kei Nakai, and Hiroyoshi Akutsu; (g) Faculty of Medicine, University of Miyazaki Hospital: Kiyotaka Yokogami, Hisao Uehara, Shiro Miyata, Gou Takeishi, Shinitsu Ryu, Toshikatsu Ikeda, Munetomo Futami, and Tetsuaki Sugimoto; (h) Graduate School of Medical and Dental Sciences, Kagoshima University: Sei Sugata, Hajime Yonezawa, Masanao Mori, and Shingo Fujio.

The efficacy and safety evaluation committee

National Cancer Center Hospital: Soichiro Shibui; Saitama Medical University Hospital: Takamitsu Fujimaki; Tokyo Metropolitan Cancer and Infectious diseases Center Komagome Hospital: Katsuyuki Karasawa.

The central pathological evaluation committee

Gunma University: Youichi Nakazato.

BCNU drug level measurement institution

Celerion Inc: Kirk Newland and Kazuko Aoyagi.

The NPC-08 study received partial financial support from the National Institute of Biomedical Innovation within the framework of the Program for Promotion of Orphan Drug/Medical Device Development. The institute provided financial support without intervening in the study.

Nobelpharma Co. Ltd. sponsored the study, providing

support for planning the protocol, monitoring, data management, statistical analysis, and many other activities in the NPC-08 study.

Conflicts of Interest Disclosure

Dr. Tomokazu Aoki is a member of the medical advisory committee of NPC-08 study and received consulting fees from Nobelpharma Co. Ltd. and an honoraria for speaking from Eisai Co. Ltd. Dr. Ryo Nishikawa is a member of the medical advisory committee of NPC-08 study and received consulting fees from Nobelpharma Co. Ltd. Dr. Nishikawa is also a member of the Avaglio study steering committee (funded by F. Hoffmann-La Roche, Ltd) and has received research funding and speaking fees from MSD KK as well as honoraria for speaking from Eisai Co. Ltd. Dr. Kazuhiko Sugiyama is a member of the medical advisory committee of NPC-08 study and received consulting fees from Nobelpharma Co. Ltd. and honoraria for speaking from Eisai Co. Ltd. Dr Masao Matsutani is a coordinating investigator of NPC-08 study, a member of the advisory committee of MSD KK, and a coordinating investigator for Chugai Pharmaceutical Co. Ltd. Dr. Matsutani also received consulting fees from Nobelpharma Co. Ltd.

The authors declare no other conflicts of interest.

References

1) Committee of Brain Tumor Registry of Japan: Report of brain tumor registry of Japan (1984–2000), 12th ed. *Neurol Med Chir (Tokyo)* 49(Suppl): S1–96, 2009
2) Brem H, Piantadosi S, Burger PC, Walker M, Selker R, Vick NA, Black K, Sisti M, Brem S, Mohr G: Placebo-controlled trial of safety and efficacy of intraoperative controlled delivery by biodegradable polymers of chemotherapy for recurrent gliomas. The Polymer-brain Tumor Treatment Group. *Lancet* 345: 1008–1012, 1995
3) Valtonen S, Timonen U, Toivanen P, Kalimo H, Kivipelto L, Heiskanen O, Unsgaard G, Kuurne T: Interstitial chemotherapy with carmustine-loaded polymers for high-grade gliomas: a randomized double-blind study. *Neurosurgery* 41: 44–48; discussion 48–49, 1997
4) Westphal M, Hilt DC, Bortey E, Delavault P, Olivares R, Warnke PC, Whittle IR, Jääskeläinen J, Ram Z: A phase 3 trial of local chemotherapy with biodegradable carmustine (BCNU) wafers (Gliadel wafers) in patients with primary malignant glioma. *Neuro Oncol* 5: 79–88, 2003
5) National Comprehensive Cancer Network (NCCN) Clinical Practice Guidelines in Oncology-v.1, 2013
6) National Cancer Institute Cancer Information Physician Data Query (May, 2012)
7) National Institute for Health and Clinical Excellence. (June, 2007)
8) Stupp R, Mason WP, van den Bent MJ, Weller M, Fisher B, Taphoorn MJ, Belanger K, Brandes AA, Marosi C, Bogdahn U, Curschmann J, Janzer RC, Ludwin SK, Gorlia T, Allgeier A, Lacombe D, Cairncross JG, Eisenhauer E, Mirimanoff RO; European Organisation for Research and Treatment of Cancer Brain Tumor and Radiotherapy Groups; National Cancer Institute of Canada Clinical Trials Group: Radiotherapy plus concomitant and adjuvant temozolomide for glioblastoma. *N Engl J Med* 352: 987–996, 2005
9) Affronti ML, Heery CR, Herndon JE, Rich JN, Reardon DA, Desjardins A, Vredenburgh JJ, Friedman AH, Bigner DD, Friedman HS: Overall survival of newly diagnosed glioblastoma patients receiving carmustine wafers followed by radiation and concurrent temozolomide plus rotational multiagent chemotherapy. *Cancer* 115: 3501–3511, 2009
10) Bock HC, Puchner MJ, Lohmann F, Schütze M, Koll S, Ketter R, Buchalla R, Rainov N, Kantelhardt SR, Rohde V, Giese A: First-line treatment of malignant glioma with carmustine implants followed by concomitant radiochemotherapy: a multicenter experience. *Neurosurg Rev* 33: 441–449, 2010
11) Larocca RV, Vitaz TW, Morassutti DJ, Doyle MJ, Glisson SD, Hargis JB, Goldsmith GH, Cervera A, Stribinskiene L, New P: A phase II study of radiation with concomitant and then sequential temozolomide (TMZ) in patients with newly diagnosed supratentorial high-grade malignant glioma who have undergone surgery with carmustine (BCNU) wafer insertion. *Neuro-oncology* 8: 391–500, 2006
12) McGirt MJ, Than KD, Weingart JD, Chaichana KL, Attenello FJ, Olivi A, Laterra J, Kleinberg LR, Grossman SA, Brem H, Quiñones-Hinojosa A: Gliadel (BCNU) wafer plus concomitant temozolomide therapy after primary resection of glioblastoma multiforme. *J Neurosurg* 110: 583–588, 2009
13) Pan E, Mitchell SB, Tsai JS: A retrospective study of the safety of BCNU wafers with concurrent temozolomide and radiotherapy and adjuvant temozolomide for newly diagnosed glioblastoma patients. *J Neurooncol* 88: 353–357, 2008
14) Jones RB, Matthes S, Shpall EJ, Fisher JH, Stemmer SM, Dufton C, Stephens JK, Bearman SI: Acute lung injury following treatment with high-dose cyclophosphamide, cisplatin, and carmustine: pharmacodynamic evaluation of carmustine. *J Natl Cancer Inst* 85: 640–647, 1993

Address reprint requests to: Tomokazu Aoki MD, PhD, Department of Neurosurgery, National Hospital Organization Kyoto Medical Center, 1-1, Fukakusa Mukaibatacho, Fushimi-ku, Kyoto, Kyoto 612-8555, Japan.
e-mail: totorolangdom@yahoo.co.jp

J Neurooncol (2011) 103:619–627
DOI 10.1007/s11060-010-0433-0

CLINICAL STUDY – PATIENT STUDY

Prediction of malignancy grading using computed tomography perfusion imaging in nonenhancing supratentorial gliomas

Takaaki Beppu · Makoto Sasaki · Kohsuke Kudo · Akira Kurose · Masaru Takeda · Hiroshi Kashimura · Akira Ogawa · Kuniaki Ogasawara

Received: 10 June 2010 / Accepted: 20 September 2010 / Published online: 15 October 2010

Abstract Tumor grade differentiation is often difficult using routine neuroimaging alone. Computed tomography perfusion imaging (CTP) provides quantitative information on tumor vasculature that closely parallels the degree of tumor malignancy. This study examined whether CTP is useful for preoperatively predicting the grade of malignancy in glioma showing no enhancement on contrast-enhanced magnetic resonance imaging (MRI). Subjects comprised 17 patients with supratentorial glioma without enhancement on MRI. CTP was performed preoperatively, and absolute values and normalized ratios of parameters were calculated. Postoperatively, subjects were classified into two groups according to histological diagnosis of grade 3 (G3) glioma or grade 2 (G2) glioma. Absolute values and normalized ratios for each parameter were compared between G3 and G2. Accuracies of normalized ratios for cerebral blood flow (*n*CBF) and cerebral blood volume (*n*CBV) in predicting a diagnosis of G3 were assessed. In addition, *n*CBV was compared between diffuse astrocytoma, G2 oligodendroglial tumor (OT), and G3 OT. Values for *n*CBF and *n*CBV differed significantly between G3 and G2. Using *n*CBV of 1.6 as a cutoff, specificity and sensitivity for distinguishing G3 were 83.3% and 90.9%, respectively. No significant difference in *n*CBV was seen between diffuse astrocytoma and G2 OT, whereas differences were noted between G2 and G3 OTs, and between diffuse astrocytoma and G3 OT. CTP offers a useful method for differentiating between G3 and G2 in nonenhancing gliomas.

Keywords Computed tomography perfusion imaging · Diffuse astrocytoma · Glioma · Nonenhancement · Oligodendroglioma · Preoperative diagnosis

T. Beppu (✉) · M. Takeda · H. Kashimura · A. Ogawa · K. Ogasawara
Department of Neurosurgery, Iwate Medical University, Uchimaru 19-1, Morioka 020-8505, Japan
e-mail: tbeppu@iwate-med.ac.jp

M. Sasaki · K. Kudo
Advanced Medical Research Center, Iwate Medical University, Morioka, Japan

A. Kurose
Department of Pathology, Iwate Medical University, Morioka, Japan

Introduction

Glioma is graded according to World Health Organization (WHO) classification, with grade 1 or 2 graded as low-grade glioma (LGG) and grade 3 or 4 commonly defined as high-grade glioma (HGG) [1]. As treatment and prognosis differ substantially between LGG and HGG, the ability to differentiate between grade 2 (G2) glioma and grade 3 (G3) glioma, as the border between LGG and HGG, is very important. On contrast-enhanced computed tomography (CT) and magnetic resonance imaging (MRI), G2 gliomas are nonenhanced due to preservation of blood–brain barrier (BBB), whereas G3 gliomas are commonly enhanced due to increased vascular permeability caused by disruption of the BBB within the tumor [2–4]. However, the relationship between histological grading and contrast enhancement on CT and MRI is not always clear. Preoperatively differentiating between G3 and G2 gliomas that are nonenhanced on conventional neuroimaging is often difficult. When patients with nonenhancing glioma are encountered, neurooncologists may perform various examinations to differentiate between G3 and G2 gliomas, such as positron emission tomography (PET) for direct assessment of tumor

metabolism, magnetic resonance spectroscopy to detect magnetic resonance signals of metabolites, and diffusion-weighted MRI to clarify structures within and surrounding the tumor. Assessment of intratumoral vasculature is one approach that may help to clarify the intratumoral biological characteristics and malignancy of a tumor, as intratumoral angiogenesis and high vascularity, which are regulated by hypoxia and various vascular endothelial growth factors, are essential for tumor growth and progression [5–7].

Angiography enables direct observation of intratumoral vessels, but is hazardous and remains limited for depiction of intratumoral microvasculature. Magnetic resonance perfusion imaging (MRP) and CT perfusion imaging (CTP) provide reliable information on the intratumoral microvasculature [8–12]. Numerous studies of perfusion imaging have shown that increasing malignancy of the glioma is associated with increased intratumoral blood volume and vascular permeability [10, 13–15]. Quantitative evaluation from perfusion imaging thus depends on both the microvasculature (vascular density and diameter), and vascular permeability due to disruption or absence of the BBB within the tumor. Previous reports have shown good correlations between findings on perfusion imaging and malignancy grading in enhancing glioma. In contrast, the BBB of vessels is preserved in nonenhancing glioma, since extravasation of contrast medium through the BBB in tumor vessels is considered to represent the main cause of tumor contrast enhancement [4]. As MRI remains the preferred technique for assessing brain tumors, studies using MRP to thoroughly evaluate gliomas greatly outnumber those using CTP, and MRP has also been applied to neurooncological applications for nonenhancing gliomas, such as determining biopsy targets and predicting malignant progression [16–18]. In recent years, CTP has gained acceptance as a valuable imaging technique for assessing hemodynamics in brain tumors [13, 14, 19–22]. However, whether CTP is useful for grading malignancy of nonenhancing gliomas remains unclear. CTP retains the advantage of a linear relationship between attenuation changes on CT and tissue concentration of contrast medium, unlike MRP [8, 20]. We therefore hypothesized that CTP should accurately provide quantitative information on only the microvasculature within the tumor, excluding extravasation due to permeability, when limited to patients with nonenhancing glioma. In the present study, we performed CTP on patients with nonenhancing glioma, and compared cerebral blood volume (CBV), cerebral blood flow (CBF), and mean transit time (MTT), as quantitative values provided from CTP, with postoperative histological diagnosis. The present study aims to determine whether CTP is useful for prediction of preoperative malignancy grading (WHO G2 or G3) in nonenhancing glioma on contrast-enhanced MRI.

Patients and methods

Patients

The study protocol was approved by the Ethics Committee of Iwate Medical University, Morioka, Japan. Consecutive patients admitted to the Department of Neurosurgery at Iwate Medical University between September 2006 and January 2010 and meeting the entry criteria were recruited to this study. Entry criteria for this study comprised: diagnosis of supratentorial glioma; tumor bulk not clearly enhanced on gadolinium-enhanced T1-weighted MRI (Gd-T1WI); tumor bulk sited in the supratentorial cerebrum; no past history relating to the brain, including surgical operation, irradiation, administration of anticancer agents or steroids, stroke, infection, or other disorders such as demyelinating disease; and provision of written informed consent to participate. Subjects comprised 17 patients (7 men, 10 women) with mean age of 47.8 years. Patient data including age, tumor site, operation method, postoperative histological diagnosis, and malignancy grade are summarized in Table 1.

Table 1 Patient summary

No.	Age (years)	Tumor site	Surgery	Histology	WHO grade
1	76	Temporal lobe	Biopsy	AA	3
2	58	Frontal lobe	Resection	AO	3
3	45	Frontal lobe	Resection	AO	3
4	34	Frontal lobe	Resection	AO	3
5	29	Frontal lobe	Resection	AO	3
6	21	Frontal lobe	Resection	AOA	3
7	78	Frontal lobe	Biopsy	DA	2
8	68	Frontal lobe	Biopsy	DA	2
9	68	Parietal lobe	Biopsy	DA	2
10	65	Frontal lobe	Resection	DA	2
11	58	Frontal lobe	Resection	DA	2
12	52	Frontal lobe	Resection	Oli	2
13	46	Temporal lobe	Resection	Oli	2
14	42	Frontal lobe	Resection	OA	2
15	30	Frontal lobe	Resection	OA	2
16	27	Frontal lobe	Resection	DA	2
17	16	Temporal lobe	Resection	OA	2

AA anaplastic astrocytoma, *AO* anaplastic oligodendroglioma, *AOA* anaplastic oligoastrocytoma, *DA* diffuse astrocytoma, *Oli* oligodendroglioma, *OA* oligoastrocytoma

Conventional MRI and CTP

Conventional MRI was performed for all subjects within 7 days before surgery. Spin-echo Gd-T1WI was performed approximately 2 min after intravenous injection of gadolinium (0.2 ml/kg, Magnevist; Bayer Schering Pharma, Berlin, Germany), using a 3.0-T whole-body scanner (GE Yokogawa Medical Systems, Tokyo, Japan) with a standard head coil. We confirmed that the tumor in each patient did not show clear enhancement with gadolinium on Gd-T1WI.

CTP was also performed within 7 days before surgery using a 16-row multidetector CT system (Aquillion 16; Toshiba Medical Systems, Tokyo, Japan), in accordance with the methods described by Sasaki et al. [23]. After performing noncontrast CT to determine the location of the tumor balk, a multislice scan targeting the tumor bulk was performed (80 kV_p; 40 mA; 1.5 s/rotation, 30 rotations field of view, 240 × 240 mm^2; four contiguous 8-mm-thick sections; total scan time, 45 s). Five seconds after intravenously injecting 40 ml (4 ml/s) nonionic iodine contrast medium (Iopamiron 300; Bayer Schering Pharma) using a power injector, dynamic scanning was started and tissue attenuation of contrast medium was monitored on a slice. Radiation doses for the scanning protocol were as follows: volume CT dose index, 150 mGy; dose–length product, 480 mGy cm; and effective dose, 1.34 mSv. Data were transferred to a commercial workstation (M900 Quadra; Ziosoft, Tokyo, Japan), and scaled color maps for CBF, CBV, and MTT were automatically created. All mathematical analyses were performed by the deconvolution method [19, 24], using CTP analysis software supplied with the workstation described above. Among the three types of deconvolution algorithms implemented in this software, we used the block-circulant singular value decomposition method. Regions of interest (ROI) for venous output and arterial input functions were manually placed at the superior sagittal sinus and a single branch of the insular segment of the middle cerebral artery on either the pathological or nonpathological side, or A2 segment of the anterior cerebral artery, respectively. ROI were also placed over the entire tumor bulk and apparently normal white matter (ANWM) on the nonpathological side, on color maps for each parameter. Size of the ROI for ANWM was established as 1.0 cm^2. In the measurement of absolute values, the vascular-pixel elimination (VPE) method was used to exclude pixels from large vessels at the cerebral surface, sulci, and cisterns [23, 25]. In the present study, we established the VPE threshold as 6.0 ml/100 g for CBV, since high-CBV areas suggesting large cortical vessels on color map disappeared satisfactorily at 6.0 ml/100 g when the threshold was varied between 5.0 and 8.0 ml/100 g using our analysis software. Large vascular pixels were thus defined as pixels with CBV values >6.0 ml/100 g and were automatically eliminated. Regional absolute values (*r*CBF, *r*CBV, and *r*MTT) were then calculated automatically for all ROI. The measurements described above were performed twice for each patient by two investigators (M.S. and K.K.) who were blinded to all clinical data, including individual patient information and histological diagnosis. Absolute values of all parameters for each patient were determined as the mean of four measured values, as determined twice by each investigator. The second test was performed 1 week after the first test, with a different randomized order of measurements from the first test. We also calculated normalized ratios (*n*CBF, *n*CBV, and *n*MTT) as the absolute value for the tumor divided by the absolute value for the ANWM for each parameter in all patients. All patients underwent surgery, with tumor resection for 13 patients and CT-guided stereotactic needle biopsy for 4 patients (Table 1). The region targeted in stereotactic biopsy was based on findings from the CBV color map. If the color map showed heterogeneous perfusion within the tumor, the targeted region corresponded to the region with the highest perfusion area for CBV. In cases with tumor resection, histological diagnosis was determined by observation at the lesion showing the most malignant histological features in all preparations. Postoperatively, histological diagnosis using specimens obtained from surgery was made by one of the investigators (A.K.) with no prior knowledge of CTP data.

Statistical analyses

All data were analyzed using PASW Statistics version 18 software (SPSS Japan, Tokyo, Japan). Inter- and intrarater reliabilities for all absolute values were evaluated according to classification of the intraclass correlation coefficient (ICC) [26]. For $ICC_{(1,1)}$ and $ICC_{(1,k)}$ as interrater reliability, agreement of all absolute values (CBF, CBV, and MTT) between first and second tests was analyzed for tumor and ANWM for each investigator, using one-factor analysis of variance (ANOVA). For $ICC_{(2,1)}$ and $ICC_{(2,k)}$ as intrarater reliability, agreement of all absolute values between the two investigators was analyzed for tumor and ANWM for each test, using two-factor ANOVA. Patients were assigned to one of two histological grading groups according to histological classification: WHO G2 or WHO G3. Frequency of biopsy was compared between G2 and G3 groups using Fisher's exact probability test. We compared absolute values from the tumor lesion for each parameter between G2 and G3 using the Mann–Whitney *U* test. Furthermore, the normalized ratio for each parameter was compared between these groups again using the Mann–Whitney *U* test. The accuracy of *r*CBF and *n*CBV in predicting a diagnosis of G3 was assessed using receiver

operating characteristic (ROC) curves. ROC curves were calculated in increments of 0.1. Absolute values and normalized ratios for CBV were compared between diffuse astrocytoma, G2 oligodendroglial tumor (OT), and G3 OT, using the Mann–Whitney U test. G2 OTs comprised oligodendroglioma or oligoastrocytoma, whereas G3 OTs comprised anaplastic oligodendroglioma or anaplastic oligoastrocytoma. Statistical significance was established at the $P < 0.05$ level in all analyses.

Results

Based on histological diagnosis after surgery, 6 patients were assigned to the G3 group and 11 patients were assigned to the G2 group (Table 1). Of these 17 patients, 4 patients underwent stereotactic biopsy. Frequency of biopsy did not differ significantly between G3 and G2 groups ($P = 0.25$).

Interrater reliability was classified as "almost perfect" for both tumor and ANWM for each investigator: $ICC_{(1,1)}$ and $ICC_{(1,k)}$ for M.S. were 0.943 and 0.971 for tumor, and 0.961 and 0.980 for ANWM, respectively, and those for K.K. were 0.966 and 0.983 for tumor, and 0.942 and 0.970 for ANWM, respectively. Intrarater reliability was also classified as "almost perfect" for both tumor and ANWM in each test: $ICC_{(2,1)}$ and $ICC_{(2,k)}$ in the first test were 0.987 and 0.993 for tumor, and 0.973 and 0.987 for ANWM, respectively, and those in the second test were 0.971 and 0.985 for tumor, and 0.973 and 0.986 for ANWM, respectively. Absolute values of tumor lesions for each parameter in G3 and G2 groups are summarized in Table 2. Absolute values for all parameters varied widely, with no significant differences in any parameters identified between G3 and G2 groups. Normalized ratios for each parameter are summarized in Table 3. Significant differences between G3 and G2 groups were identified for nCBF and nCBV, with no significant differences in nMTT.

The cutoff for accuracy was defined as the point lying closest to the upper-left corner of the ROC curve.

Table 2 Absolute values for each parameter

	rCBF (ml/100 g/min)	rCBV (ml/100 g)	rMTT (s)
G3 ($n = 6$)			
Range	10.8–27.0	1.9–3.2	6.8–10.8
Mean ± SD	18.3 ± 5.3	2.5 ± 0.5	8.5 ± 1.5
G2 ($n = 11$)			
Range	8.8–23.3	1.3–2.6	7.0–12.2
Mean ± SD	15.5 ± 4.2	2.1 ± 0.4	8.8 ± 1.5
P	0.27	0.25	0.76

SD standard deviation

Table 3 Normalized ratios for each parameter

	nCBF	nCBV	nMTT
G3 ($n = 6$)			
Range	1.34–3.00	1.54–2.39	0.76–1.06
Mean ± SD	2.10 ± 0.57	1.92 ± 0.37	0.90 ± 0.12
G2 ($n = 11$)			
Range	0.92–2.00	0.91–1.75	0.79–1.07
Mean ± SD	1.41 ± 0.38	1.26 ± 0.28	0.91 ± 0.09
P	0.01	0.004	0.76

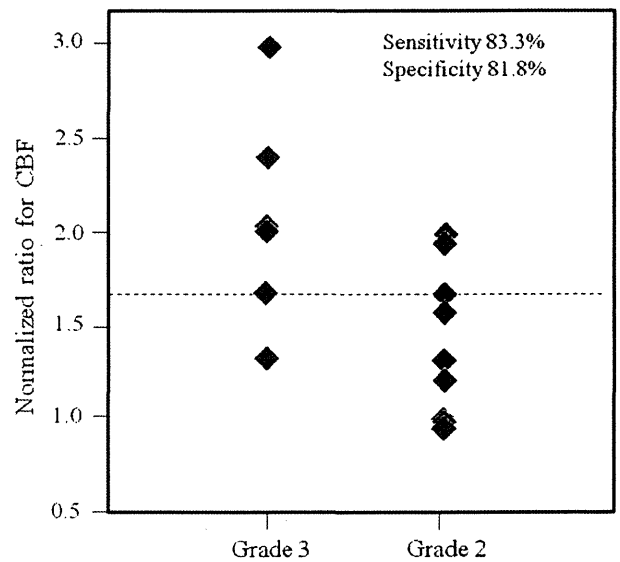

Fig. 1 Relationship between nCBF value and WHO grading. Using a cutoff of 1.7 (*dashed line*), nCBV was ≥1.7 for 5 (83.3%) of 6 patients with G3, compared with <1.7 for 9 (63.6%) of 11 patients with G2

Sensitivity and specificity in predicting a diagnosis of G3 were 83.3% and 81.8% for nCBF (cutoff 1.7), and 83.3% and 90.9% for nCBV (cutoff 1.6) (Figs. 1, 2). Accuracy for predicting a diagnosis of G3 was higher with nCBV than with nCBF.

A comparison of nCBV was made between G3 OT, G2 OT, and diffuse astrocytoma (Table 4). Significant differences in nCBV were identified between G3 and G2 OTs ($P = 0.009$), and between G3 OT and diffuse astrocytoma ($P = 0.02$), whereas no significant difference was seen between G2 OT and diffuse astrocytoma ($P = 0.36$).

Illustrative cases

We now describe the cases of two patients for whom CTP provided useful information for predicting tumor grading. Gd-T1WI for case 6 showed glioma with no clear enhancement in the right frontal lobe (Fig. 3a). Using the

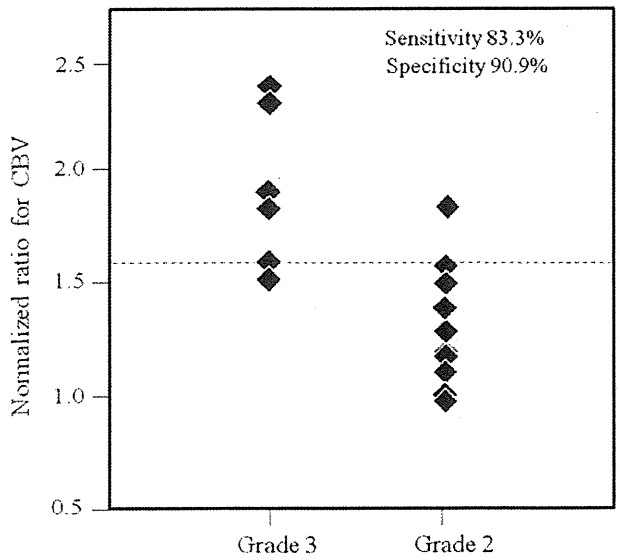

Fig. 2 Relationship between *n*CBV value and WHO grading. Using a cutoff point of 1.6 (*dashed line*), *n*CBV was ≥1.6 for 5 (83.3%) of 6 patients with G3 and <1.6 for 10 (90.9%) of 11 patients with G2

Table 4 Normalized ratio (mean ± SD) for CBV in G3 OT, G2 OT, and diffuse astrocytoma

	*n*CBV
G3 OT ($n = 5$)	1.99 ± 0.36
G2 OT ($n = 5$)	1.16 ± 0.24
Diffuse astrocytoma ($n = 6$)	1.35 ± 0.31

OT oligodendroglial tumors

VPE method, color mapping of CBV demonstrated large vessels of the cerebral surface to be successfully excluded (Fig. 3b). Color mapping of CBV depicted areas of hyperperfusion within the tumor. The *n*CBV for this case (*n*CBV = 2.3) was higher than the cutoff point. Tissue specimens obtained from gross total resection showed typical histological features of G3 anaplastic oligoastrocytoma.

Gd-T1WI for case 14 showed nonenhancing glioma of the right frontal lobe (Fig. 4a). The VPE method satisfactorily eliminated large vessels of the cerebral surface (Fig. 4b). On color mapping, areas of hyperperfusion seemed to be minor compared with those in case 6. The *n*CBV in this case (*n*CBV = 1.2) was lower than the cutoff point. After tumor resection, histological diagnosis was G2 oligoastrocytoma.

Discussion

Previous reports have documented that G3 gliomas make up 40–46% of nonenhancing gliomas on conventional MRI [3, 4]. Our finding of G3 tumors in 6 (35.2%) of 17 patients

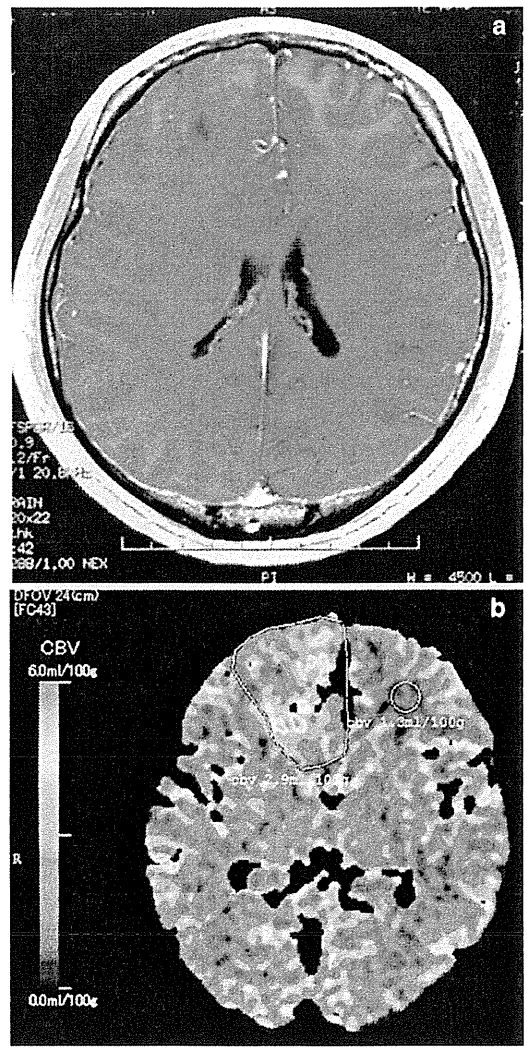

Fig. 3 Gd-T1WI (**a**) and color map of CBV (**b**) for case 6. *Circle* ROI covering the entire tumor bulk and ANWM localized on the nonpathological side

was close to this level. Thus, preoperative differentiation between G3 and G2 using MRI is often difficult. Biopsy or resection allowing histological diagnosis currently remain the basis for differentiation between G3 and G2 gliomas. However, neuroimaging can provide useful information on pathological diagnosis, particularly for patients who do not undergo biopsy or resection allowing histological diagnosis. Novel neuroimaging procedures other than routine MRI are thus desired. CTP and MRP provide reliable information on tumor vasculature, which can help to determine the extent of malignancy in glioma [8, 10, 22]. Although limitations of CTP include radiation dose and limited area of coverage compared with MRP, the linear relationship between attenuation changes on CT and tissue concentration of contrast medium and the lack of confounding sensitivity to flow artifacts allow CTP to

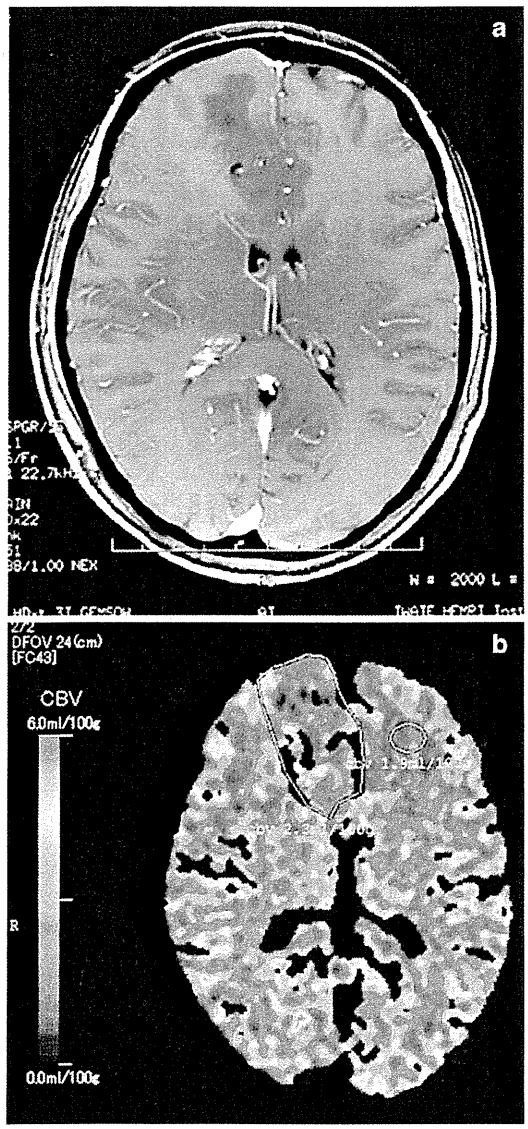

Fig. 4 Gd-T1WI (**a**) and color map of CBV (**b**) for case 14. *Circle* ROI covering the entire tumor bulk and ANWM localized on the nonpathological side

potentially offer a more accurate representation of tissue microvasculature than similar MRP studies [8, 20]. Furthermore, CTP offers advantages such as measurement of quantitative absolute values, greater availability, fast scanning time, high spatial resolution, low cost, and the ability to use this technique for patients who cannot undergo MRI due to the presence of metallic materials in the body [14, 22, 27].

CBF derived from CTP has been suggested to show a tendency toward overestimation, compared with that derived from PET [28]. Since overestimation of CBF in CTP was attributable to the presence of large vessels on the cerebral surface, as contrast materials act as a nondiffusible intravascular tracer in CTP unlike in PET, the VPE method has been proposed to eliminate flow in large vessels [25]. Accurate measurement of CBV contributes to accurate CBF and MTT, as these parameters are closely associated in the central volume principle as CBF = CBV/MTT [29]. We therefore used the VPE method in the present study. We think that optimal threshold differs according to the specific analysis software used for CTP. While VPE threshold was 8.0 ml/100 g in the report by Kudo et al. [25], we established a threshold of 6.0 ml/100 g, since high-CBV areas from cortical large vessels disappeared satisfactorily at this threshold for the analysis software used in our study. Another reason for using the VPE method is that OTs are commonly seen as superficially located tumors in the brain [30, 31]. Elimination of superficial large vessels at the cerebral surface, sulci, and cisterns thus seems warranted when CTP is performed for OTs.

In previous reports of CTP, *r*CBV values ranged from 2.3 to 8.87 ml/100 g for HGG and from 0.95 to 3.28 ml/100 g for LGG, differing significantly between HGG and LGG [13, 14, 20]. The present mean rCBV values in G3 and G2 (Table 2) agreed with previous findings. In addition, mean rCBV values in both G3 and G2 were less than half of 6.0 ml/100 g as VPE threshold. These findings suggest that the VPE method used in this study did not exclude tumor vessels along with other large vessels from CBV maps. While *r*CBV for G3 tended to be on the low side compared with previous reports, this could have resulted from the exclusion of patients with enhancing glioma as subjects in this study. Extravasation of contrast medium through the BBB in enhanced glioma may directly lead to increased CBV, due to the linear relationship between attenuation changes on CT and tissue concentration of contrast medium. Jain et al. [20] documented that *r*CBF and *r*CBV in nonenhancing G3 glioma do not differ significantly from those in nonenhancing G2 glioma, although sample size in that report was small. The present study with more subjects suggested that even nonenhancing G3 glioma retains more vascular density than G2, although the difference in *r*CBV between the two groups was minor (Table 2). However, this result might have been influenced by the disproportionate number of OTs in the G2 (42%) and G3 (83%) groups. If vascular density is significantly higher in G3 OT than in anaplastic astrocytoma, the large number of G3 OTs may have result in a high mean CBV for the G3 group in this study. This issue represents a definite limitation to the present study.

Concentration of contrast medium within the tumor might be subtly influenced by individual parameters such as body size and cardiac output volume, and differences in analytical software among institutes. We must emphasize the importance of estimation using normalized ratios, as

this allows us to ignore these differences. Ellika et al. [22] reported findings for *n*CBV using CTP in 19 patients with glioma, composed of a mixture of enhancing and nonenhancing WHO G1–G4 gliomas, and the utility of *n*CBF and *n*CBV for distinguishing HGG from LGG. They also documented *n*CBF and *n*CBV ranges of 0.78–3.75 and 1.5–3.7 in two patients with nonenhancing G3 glioma, and ranges of 1.26–1.48 and 0.94–1.72 in three patients with nonenhancing G2 glioma, respectively. Mean values of *n*CBF and *n*CBV in G3 and G2 in this study (Table 3) seemed close to the values reported by Ellika et al.

Radiographic grading of gliomas with conventional MRI is not always accurate, with 85.7% sensitivity for predicting HGG, even when including subjects with enhancing glioma [22]. When subjects are limited to those with nonenhancing gliomas, radiographic grading using conventional MRI should be more difficult. A previous report documented 85.7% sensitivity and 100% specificity for identifying HGG using *n*CBV [22]. In the present study, CTP could distinguish nonenhancing G3 glioma from nonenhancing G2 glioma with 83.3% sensitivity and 90.9% specificity using *n*CBV (Fig. 2). This was superior to the results for *n*CBF. Accuracy for distinguishing G3 using *n*CBV in the present study was by no means inferior to that reported by Ellika et al. [22], but subjects in this study were limited to those with nonenhancing glioma. These results suggest that *n*CBV in CTP is useful as an auxiliary examination in addition to routine neuroimaging for predicting the grade of malignancy in nonenhancing gliomas.

Previous studies using MRP have documented higher relative CBV in OT than in other gliomas [32–34]. Lev et al. [33] suggested that OTs tend to appear as high blood volume lesion on MRP, without respect to tumor grade. Two reports using MRP documented that G2 OTs show higher relative CBV than diffuse astrocytoma [32, 34]. Also in a report using CTP by Narang et al. [15], G2 OTs showed a trend towards higher CBV than G2 astrocytic tumors, although no significant difference was found, and no significant difference in CBV between G3 OTs and G2 OTs was identified. Those reports explained the high relative CBV of OT by a hypothesis based on the specific histological features of fine capillary networks [33]. Furthermore, those reports suggested that grading malignancy may be difficult when patients with OT are included, due to a high relative CBV. In the present study, no significant difference in *n*CBV was seen between diffuse astrocytoma and G2 OT, whereas significant differences were found between G3 OT and G2 OT. The difference between the reports described above and the present investigation might be explained by differences between MRP and CTP, and by the use of the VPE method in this study. Signal changes in dynamic susceptibility contrast (DSC) MRI for MRP do not depend on only the concentration of contrast material, but also on T2* or T2 relaxation rates, which are affected by calcified foci and hemorrhage within tumor tissue. These histological features are commonly seen in OTs. DSC signals might thus be higher in OTs than in diffuse astrocytoma, even when the microvascular densities are comparable. The VPE method may have eliminated pixels of high-CBV vessels in OTs, if vascular density in OTs is significantly higher than that in diffuse astrocytoma. However, exclusion of large vessels at the cerebral surface and sulci from CTP maps is important, as OTs grow superficially in the brain. Cha et al. [32] explained for reason of high relative CBV for OTs in MRP by the predominant cortical location in addition to distinct vascular pattern in OTs. We think that CTP with the VPE method is useful for simple malignancy grading in subjects with OTs. Conversely, MRP offers potential advantages for the diagnosis of OTs. However, CTP should not be performed additionally to MRP if the purpose in examination is achieved by MRP, as CTP retains drawbacks such as radiation dose and iodine contrast medium.

The present study possesses some limitations regarding the interpretation of study results. First, the number of patients in this study was small, with remarkably fewer cases of anaplastic astrocytoma compared with OT in G3, as mentioned above. Further investigation including a larger number of cases of anaplastic astrocytoma is needed. A second limitation is the possible discrepancy between histological diagnosis and the region of highest CBV within the tumor. The region targeted for stereotactic biopsy was not rigorously transferred from the region of highest *r*CBV ("hot spots"). However, risk of histological misdiagnosis caused by sampling error during biopsy might be negligible, since the number of patients who underwent biopsy was small in both G3 and G2, and no significant difference in frequency of biopsy was seen between groups. In patients who underwent tumor resection, histological diagnosis was not made using tissue specimens rigorously corresponding to "hot spots." However, histological diagnosis based on the most malignant histological features should be closely associated with high CBV, as increased malignancy is associated with higher vascular density. CTP with a 16-row multidetector CT scanner, covering only four contiguous 8-mm-thick sections, did not cover the entire tumor bulk in some patients. For those patients, histological diagnosis was made using tumor tissues corresponding to the area depicted in CTP. A third limitation was that data calculated from CTP in this study were not the highest CBV values for a small ROI placed in "hot spots" on a color map, but rather were mean values for a large ROI covering the entire tumor bulk. This issue also influences the second limitation. We thought that the simple protocol in this study, combining absolute values as a mean in a large ROI with histological diagnosis from the

area of the most malignant features, is suitable for application in clinical practice, as tissue sampling error of regions corresponding to a small ROI can be avoided. High ICC in inter- and intrarater reliabilities showed that the protocol used in this study offers high reproducibility.

Conclusions

We performed CTP combined with the VPE method for 17 patients, to clarify whether CTP can accurately differentiate between G3 and G2 nonenhancing glioma. Our results showed that *n*CBV from CTP was highly accurate in differentiating G3 from G2 nonenhancing gliomas. The most important result was that CTP enabled differentiation between G3 and G2 nonenhancing OTs. CTP combined with the VPE method offers a useful technique for differentiating between G3 and G2 in nonenhancing gliomas.

Acknowledgments This study was supported in part by a Grant-in-Aid for Advanced Medical Science Research from the Ministry of Science, Education, Sports, and Culture, Japan.

References

1. Louis DN, Ohgaki H, Wiestler OD, Cavenee WK, Burger PC, Jouvet A, Scheithauer BW, Kleihues P (2007) The 2007 WHO classification of tumours of the central nervous system. Acta Neuropathol 114:97–109
2. Dean BL, Drayer BP, Bird CR, Flom RA, Hodak JA, Coons SW, Carey RG (1990) Gliomas: classification with MR imaging. Radiology 174:411–415
3. Ginsberg LE, Fuller GN, Hashmi M, Leeds NE, Schomer DF (1998) The significance of lack of MR contrast enhancement of supratentorial brain tumors in adults: histopathological evaluation of a series. Surg Neurol 49:436–440
4. Mihara F, Numaguchi Y, Rothman M, Kristt D, Fiandaca M, Swallow L (1995) Non-enhancing supratentorial malignant astrocytomas: MR features and possible mechanisms. Radiat Med 13:11–17
5. Jain RK, Gerlowski LE (1986) Extravascular transport in normal and tumor tissues. Crit Rev Oncol Hematol 5:115–170
6. Shweiki D, Itin A, Soffer D, Keshet E (1992) Vascular endothelial growth factor induced by hypoxia may mediate hypoxia-initiated angiogenesis. Nature 359:843–845
7. Vajkoczy P, Menger MD (2000) Vascular microenvironment in gliomas. J Neurooncol 50:99–108
8. Barnett G (2006) High-grade gliomas. Humana, Totowa
9. Law M, Cha S, Knopp EA, Johnson G, Arnett J, Litt AW (2002) High-grade gliomas and solitary metastases: differentiation by using perfusion and proton spectroscopic MR imaging. Radiology 222:715–721
10. Law M, Yang S, Wang H, Babb JS, Johnson G, Cha S, Knopp EA, Zagzag D (2003) Glioma grading: sensitivity, specificity, and predictive values of perfusion MR imaging and proton MR spectroscopic imaging compared with conventional MR imaging. Am J Neuroradiol 24:1989–1998
11. Eastwood JD, Lev MH, Provenzale JM (2003) Perfusion CT with iodinated contrast material. Am J Roentgenol 180:3–12
12. Hoeffner EG, Case I, Jain R, Gujar SK, Shah GV, Deveikis JP, Carlos RC, Thompson BG, Harrigan MR, Mukherji SK (2004) Cerebral perfusion CT: technique and clinical applications. Radiology 231:632–644
13. Ding B, Ling HW, Chen KM, Jiang H, Zhu YB (2006) Comparison of cerebral blood volume and permeability in preoperative grading of intracranial glioma using CT perfusion imaging. Neuroradiology 48:773–781
14. Eastwood JD, Provenzale JM (2003) Cerebral blood flow, blood volume, and vascular permeability of cerebral glioma assessed with dynamic CT perfusion imaging. Neuroradiology 45:373–376
15. Narang J, Jain R, Scarpace L, Saksena S, Schultz LR, Rock JP, Rosenblum M, Patel SC, Mikkelsen T (2010) Tumor vascular leakiness and blood volume estimates in oligodendrogliomas using perfusion CT: an analysis of perfusion parameters helping further characterize genetic subtypes as well as differentiate from astroglial tumors. J Neurooncol. doi:10.1007/s11060-010-0317-3
16. Maia AC Jr, Malheiros SM, da Rocha AJ, Stavale JN, Guimaraes IF, Borges LR, Santos AJ, da Silva CJ, de Melo JG, Lanzoni OP, Gabbai AA, Ferraz FA (2004) Stereotactic biopsy guidance in adults with supratentorial nonenhancing gliomas: role of perfusion-weighted magnetic resonance imaging. J Neurosurg 101:970–976
17. Danchaivijitr N, Waldman AD, Tozer DJ, Benton CE, Brasil Caseiras G, Tofts PS, Rees JH, Jager HR (2008) Low-grade gliomas: do changes in rCBV measurements at longitudinal perfusion-weighted MR imaging predict malignant transformation? Radiology 247:170–178
18. Price SJ (2010) Advances in imaging low-grade gliomas. Adv Tech Stand Neurosurg 35:1–34
19. Nabavi DG, Cenic A, Craen RA, Gelb AW, Bennett JD, Kozak R, Lee TY (1999) CT assessment of cerebral perfusion: experimental validation and initial clinical experience. Radiology 213: 141–149
20. Jain R, Ellika SK, Scarpace L, Schultz LR, Rock JP, Gutierrez J, Patel SC, Ewing J, Mikkelsen T (2008) Quantitative estimation of permeability surface-area product in astroglial brain tumors using perfusion CT and correlation with histopathologic grade. Am J Neuroradiol 29:694–700
21. Jain R, Scarpace L, Ellika S, Schultz LR, Rock JP, Rosenblum ML, Patel SC, Lee TY, Mikkelsen T (2007) First-pass perfusion computed tomography: initial experience in differentiating recurrent brain tumors from radiation effects and radiation necrosis. Neurosurgery 61:778–786
22. Ellika SK, Jain R, Patel SC, Scarpace L, Schultz LR, Rock JP, Mikkelsen T (2007) Role of perfusion CT in glioma grading and comparison with conventional MR imaging features. Am J Neuroradiol 28:1981–1987
23. Sasaki M, Kudo K, Ogasawara K, Fujiwara S (2009) Tracer delay-insensitive algorithm can improve reliability of CT perfusion imaging for cerebrovascular steno-occlusive disease: comparison with quantitative single-photon emission CT. Am J Neuroradiol 30:188–193
24. Wintermark M, Maeder P, Thiran JP, Schnyder P, Meuli R (2001) Quantitative assessment of regional cerebral blood flows by perfusion CT studies at low injection rates: a critical review of the underlying theoretical models. Eur Radiol 11:1220–1230
25. Kudo K, Terae S, Katoh C, Oka M, Shiga T, Tamaki N, Miyasaka K (2003) Quantitative cerebral blood flow measurement with dynamic perfusion CT using the vascular-pixel elimination method: comparison with H2(15)O positron emission tomography. Am J Neuroradiol 24:419–426
26. Shrout PE, Fleiss JL (1979) Intraclass correlations: uses in assessing rater reliability. Psychol Bull 86:420–428
27. Miles KA, Charnsangavej C, Lee FT, Fishman EK, Horton K, Lee TY (2000) Application of CT in the investigation of angiogenesis in oncology. Acad Radiol 7:840–850

28. Gillard JH, Minhas PS, Hayball MP, Bearcroft PW, Antoun NM, Freer CE, Mathews JC, Miles KA, Pickard JD (2000) Assessment of quantitative computed tomographic cerebral perfusion imaging with H2(15)O positron emission tomography. Neurol Res 22: 457–464
29. Meier P, Zierler KL (1954) On the theory of the indicator-dilution method for measurement of blood flow and volume. J Appl Physiol 6:731–744
30. Piepmeier J, Baehring JM (2004) Surgical resection for patients with benign primary brain tumors and low grade gliomas. J Neurooncol 69:55–65
31. Beppu T, Inoue T, Nishimoto H, Ogasawara K, Ogawa A, Sasaki M (2007) Preoperative imaging of superficially located glioma resection using short inversion-time inversion recovery images in high-field magnetic resonance imaging. Clin Neurol Neurosurg 109:327–334
32. Cha S, Tihan T, Crawford F, Fischbein NJ, Chang S, Bollen A, Nelson SJ, Prados M, Berger MS, Dillon WP (2005) Differentiation of low-grade oligodendrogliomas from low-grade astrocytomas by using quantitative blood-volume measurements derived from dynamic susceptibility contrast-enhanced MR imaging. Am J Neuroradiol 26:266–273
33. Lev MH, Ozsunar Y, Henson JW, Rasheed AA, Barest GD, Harsh GR IV, Fitzek MM, Chiocca EA, Rabinov JD, Csavoy AN, Rosen BR, Hochberg FH, Schaefer PW, Gonzalez RG (2004) Glial tumor grading and outcome prediction using dynamic spin-echo MR susceptibility mapping compared with conventional contrast-enhanced MR: confounding effect of elevated rCBV of oligodendrogliomas. Am J Neuroradiol 25:214–221
34. Maia AC Jr, Malheiros SM, da Rocha AJ, da Silva CJ, Gabbai AA, Ferraz FA, Stavale JN (2005) MR cerebral blood volume maps correlated with vascular endothelial growth factor expression and tumor grade in nonenhancing gliomas. Am J Neuroradiol 26:777–783

Mol Imaging Biol (2013)
DOI: 10.1007/s11307-013-0670-7

RESEARCH ARTICLE

Standardized Uptake Value in High Uptake Area on Positron Emission Tomography with ^{18}F-FRP170 as a Hypoxic Cell Tracer Correlates with Intratumoral Oxygen Pressure in Glioblastoma

Takaaki Beppu,[1] Kazunori Terasaki,[2] Toshiaki Sasaki,[2] Shunrou Fujiwara,[1] Hideki Matsuura,[1] Kuniaki Ogasawara,[1] Koichiro Sera,[2] Noriyuki Yamada,[3] Noriyuki Uesugi,[3] Tamotsu Sugai,[3] Kohsuke Kudo,[4] Makoto Sasaki,[4] Shigeru Ehara,[5] Ren Iwata,[6] Yoshihiro Takai[7]

[1]*Department of Neurosurgery, Iwate Medical University, Uchimaru 19-1, Morioka 020-8505, Japan*
[2]*Cyclotron Research Center, Iwate Medical University, Morioka, Japan*
[3]*Department of Clinical Pathology, Iwate Medical University, Morioka, Japan*
[4]*Institute for Biomedical Sciences, Iwate Medical University, Morioka, Japan*
[5]*Department of Radiology, Iwate Medical University, Morioka, Japan*
[6]*Cyclotron and Radioisotope Center (CYRIC), Tohoku University, Sendai, Japan*
[7]*Department of Radiology and Radiation Oncology, Hirosaki University Graduate School of Medicine, Hirosaki, Japan*

Abstract

Purpose: The aim of this study was to clarify the reliability of positron emission tomography (PET) using a new hypoxic cell tracer, 1-(2-[^{18}F]fluoro-1-[hydroxymethyl]ethoxy)methyl-2-nitroimidazole (^{18}F-FRP170).

Procedures: Twelve patients with glioblastoma underwent ^{18}F-FRP170 PET before tumor resection. Mean standardized uptake value (SUV) and normalized SUV were calculated at regions within a tumor showing high (high-uptake area) and relatively low (low-uptake area) accumulations of ^{18}F-FRP170. In these areas, intratumoral oxygen pressure (tpO_2) was measured using microelectrodes during tumor resection.

Results: Mean tpO_2 was significantly lower in the high-uptake area than in the low-uptake area. A significant negative correlation was evident between normalized SUV and tpO_2 in the high-uptake area.

Conclusion: The present findings suggest that high accumulation on ^{18}F-FRP170 PET represents viable hypoxic tissues in glioblastoma.

Key words: F-FRP170, PET, Hypoxia, Glioblastoma, Oxygen pressure, HIF1-α

Abbreviation: Cu-ATSM, ^{64}Cu-diacetyl-bis(N4-methylthiosemicarbazone); ^{18}F-FRP170, 1-(2-[^{18}F]fluoro-1-[hydroxymethyl]ethoxy)methyl-2-nitroimidazole; ^{18}F-FAZA, 1-α-D-(5-deoxy-5-[^{18}F]-fluoroarabinofuranosyl)-2-nitroimidazole; ^{18}F-FMISO, [^{18}F]fluoromisonidazole; Gd-T1WI, Gadolinium-enhanced T1-weighted imaging; HIF, Hypoxic-inducible factor; MRI, Magnetic resonance imaging; ROI, Region of interest; T2WI, T2-weighted imaging; PET, Positron emission tomography; VEGF, Vascular endothelial growth factor

Correspondence to: Takaaki Beppu; *e-mail:* tbeppu@iwate-med.ac.jp

Published online: 20 July 2013